Design of Photonics Crystal Fiber Sensors for Bio-medical Applications

Santosh Kumar*[a], Akanksha Bisht[a], Ashish Bisht[a], Gurdeep Singh[a], Angela Amphawan[b]
[a]Department of Electronics & Comm. Engineering, DIT University, Dehradun-248009, India;
[b]Fulbright Research Fellow, Massachusetts Institute of Technology, 02139 Cambridge, Massachusetts, USA; [b]InterNetWorks Research Laboratory, School of Computing, Universiti Utara Malaysia, 06010 Sintok, Kedah, Malaysia

ABSTRACT

Photonic Crystal Fibers (PCFs) have special structures and offer a number of novel design options, such as very large or very small mode areas, high numerical aperture, guidance of light in air, and novel dispersion properties. PCFs have become an attractive field for the researchers and they are trying to work on these to get their properties applied in dispersion related applications, sensing applications and much more. PCFs sensors are widely used in bio-medical applications. The sensitivity and performance of sensors are enhanced due to novel applications of PCFs. This paper outlines a novel design for a generalized biomedical sensor by collaborating PCF and electro-optic effect of Lithium Niobate ($LiNbO_3$) based Mach-Zehnder interferometer (MZI) structure.

Keywords: Photonic crystal fibers; biomedical sensors; lithium niobate; beam propagation method.

1. INTRODUCTION

Photonic crystal fibers are considered as one of the most encouraging elements in optical biosensors due to their enriched performance capacities of being immune to electromagnetic noise, reliable and highly sensitive in comparison with already existing optic fibre biosensors. The sensing application of PCF was first noticed in [1], where absorption spectrum of acetylene filled waveguide was studied. A photonic crystal based sensor allowing detection of individual molecules via their two-photon fluorescence has been described in [2]. PCFs can be used for evanescent-wave sensing of bio molecules, such as DNA or proteins [3-4]. The latest advances in PCFs and micro electro mechanical system (MEMS) offer considerable opportunity to realize an optical endoscope which permits high-resolution visualization of internal organs of body [5-7]. The use of polymer optical fibres permits remarkable composition flexibility of waveguide and sensing features [8]. The polarization-maintaining photonic crystal fiber (PM-PCF) with higher birefringence than already existing polarization-maintaining fibers, allows a smaller length in practical use [9]. Optical switching phenomena using MZIs and its efficient application to perform various digital logic operations in [10-14].

In this paper, a novel generalized biomedical sensor is proposed by collaborating photonic crystal fiber and electro-optic effect of Lithium Niobate ($LiNbO_3$) based MZI structure. The proposed device is based on the fact that effective refractive index of a PCF varies on selectively filling the holes of a normal index-guiding solid core. The proposed device is pumped with a 635 nm signal and the return photoluminescence is coupled to the active surface of a light

Optical Measurement Systems for Industrial Inspection IX, edited by Peter Lehmann, Wolfgang Osten, Armando Albertazzi G. Jr., Proc. of SPIE Vol. 9525, 95252B

dependent resistor (LDR), which is connected as one of the four arms of wheat stone bridge. The potential difference generated across the wheat stone bridge is applied to inputs of a differential amplifier, output of which is applied to second electrode of MZI. Section 2 explains the working principle of the experimental set up.

2. WORKING PRINCIPLE OF EXPERIMENTAL SETUP

Figure 1 shows the experimental set up for the proposed device. A gap is created originally in between two single mode fibers of 2 μm length each. After that, a photonic crystal fiber of 2 μm length with the body fluid (e.g. blood, urine, sweat, saliva, sputum etc.) inserted in its holes is fixed in the slot. The optical output obtained at the end of single mode fiber-2 is applied to the active surface area of a light dependent resistor (LDR), whose resistance depends on intensity of incident light. The LDR is connected as one of the arm of wheat stone bridge. A battery source is connected across wheat stone bridge, so as to create a potential difference between points P_1 and P_2. Points P_1 and P_2 are connected to respective inputs of a differential amplifier, whose output is applied to second electrode of an MZI. The parameters of differential amplifier are adjusted in such a way that as concentration level of a particular salt exceeds the specified limit, light signal obtained at output of MZI switches from one port to the other.

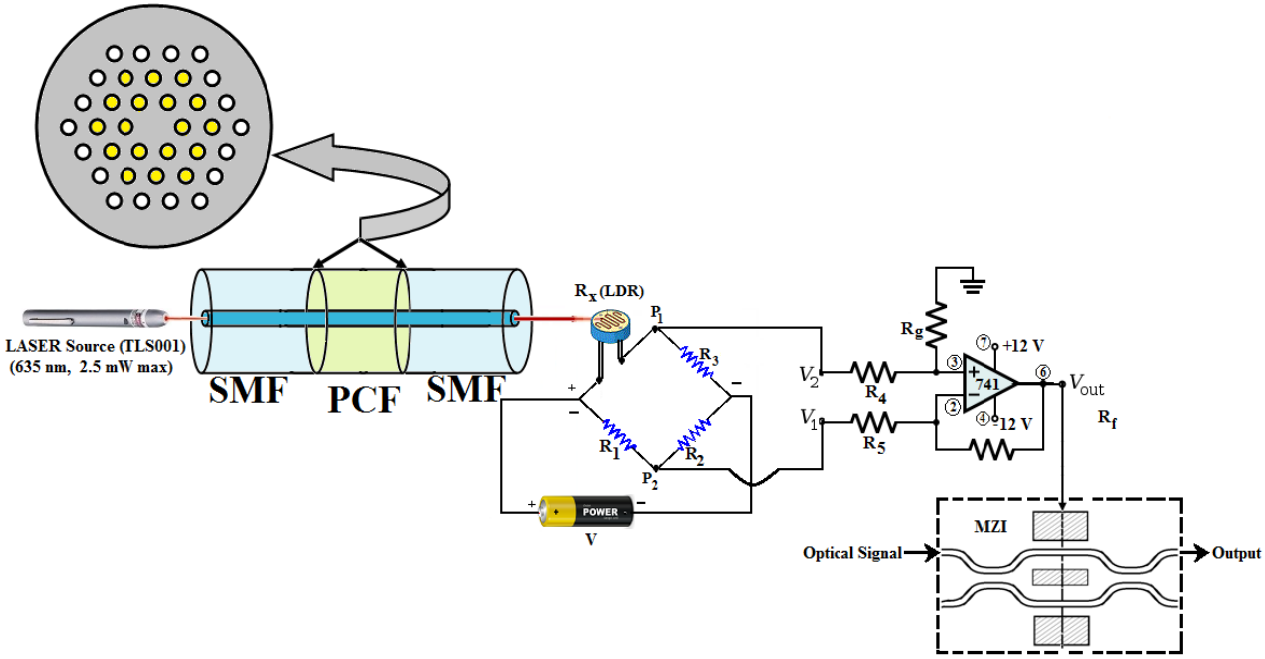

Fig. 1: Schematic diagram for experimental set up for a generalized bio-medical sensor.

2.1 Design of uric acid concentration sensor

Uric acid is a by-product of the metabolic breakdown of purines, which are found in some foods and drinks. Most of the uric acid dissolves in blood and reaches to the kidneys. From there it passes out in urine. If the body produces too much uric acid or is not able to remove most of it, many medical conditions like formation of ammonium acid urate kidney stones, diabetes and gout can be found. In this Section, design of uric acid concentration sensor using various blood

specimens is discussed. The experimental set-up for the proposed sensor is shown in Fig. 1, except that instead of generalizing the sensor for different applications, air holes of the PCF are filled with a serum specimen. A laser source with a wavelength of 635 nm has been used to generate a beam of light, and then this beam is guided into PCF using a SMF. On filling up the air holes with serum specimens taken from different persons, electric field intensity monotonically decreases with the increase in concentration of uric acid as shown in Fig. 2.

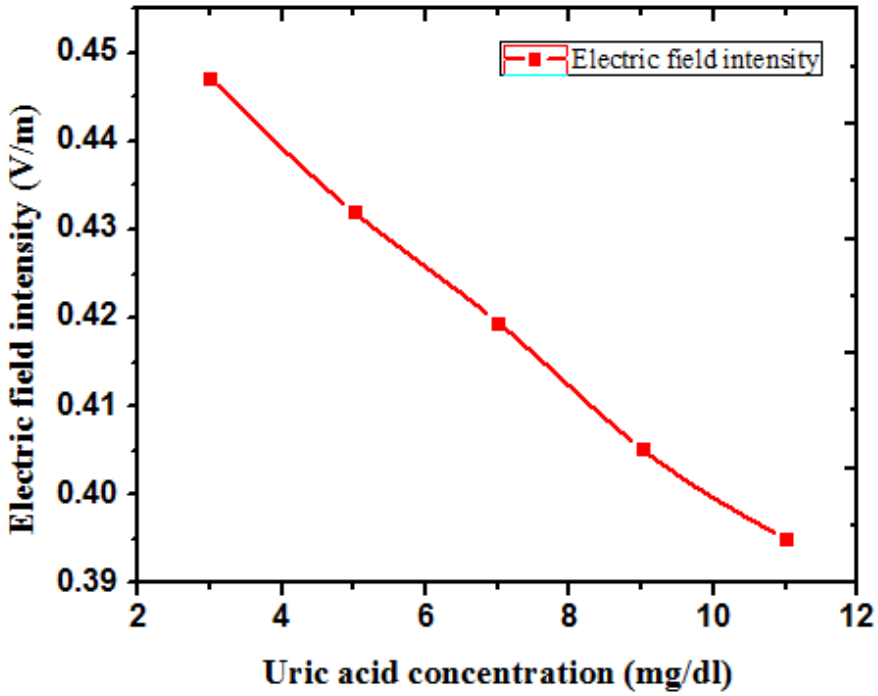

Fig. 2: Variation of electric field intensity with respect to uric acid concentration (obtained at output of PCF).

Light obtained from PCF is incident on an LDR, which is connected as one of the arm of wheat stone bridge. The resistance of LDR decreases as the illuminance ($E_{v(lx)}$) increases. The illuminance ($E_{v(lx)}$) is given by the relation

$$E_{v(lx)} = P_w \times \eta_{lm/w} / A_{m^2} \quad (1)$$

$\eta_{\frac{lm}{w}}$ = 150 lm/W for laser source operating at 635nm.

A_{m^2} is the surface area over which the light is incident. A_{m^2}=1.9625×$10^{-05} m^2$ for the LDR used in the experimental setup. The relation between illuminance and resistance of an LDR is given by

$$\frac{E_v}{E_{vo}} = \left(\frac{R}{R_0}\right)^A \quad (2)$$

E_{vo} and R_0 are the reference values for illuminace and resistance respectively, values of which are 1000 lux and 400 Ω respectively for the LDR used in our experimental setup. A is in the range from -0.7 to -0.9. So, the resistance of LDR

increases with decrease in illuminance as obtained from Eqn. 2. Figure 3 shows the variation of resistance for LDR with increase in uric acid concentration in serum.

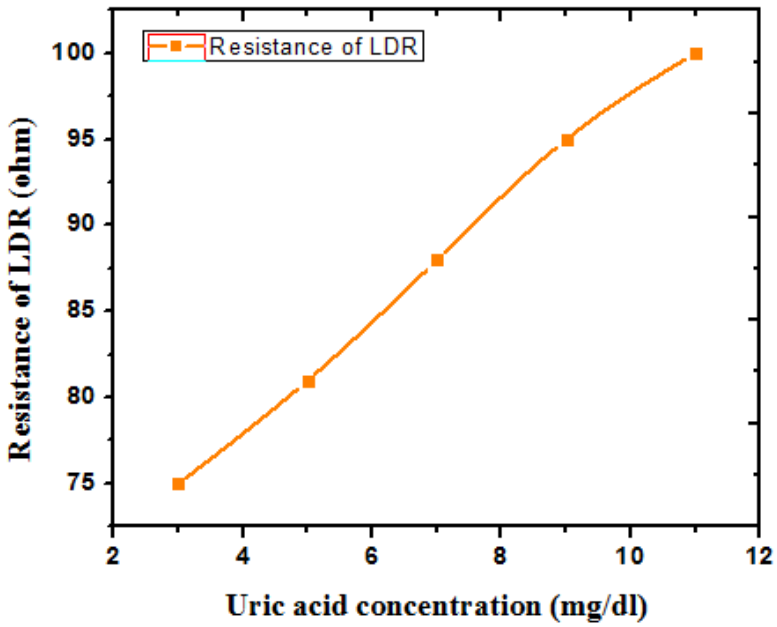

Fig. 3: Graph showing variation of resistance of LDR with increase in uric acid concentration.

When the concentration of uric acid is 3 mg/dl, resistance of LDR is equal to75Ω. Resistances R_1, R_2 and R_3 are selected in such a way that a null condition is achieved in wheat stone bridge (i.e. 0 Volt potential difference exists between points P_1 and P_2). This 0 Volt potential is applied to second electrode of MZI [15] via a differential amplifier. As the resistance of LDR varies (i.e. uric acid concentration increases), wheat stone bridge gets unbalanced and a finite voltage difference is applied to input of differential amplifier, which amplifies the voltage difference (as shown in Table1) according to the relation.

$$V_{out} = \frac{R_f}{R_4}(V_2 - V_1) \tag{3}$$

Figure 4 shows the voltage obtained at output of differential amplifier with respect to resistance of LDR. When the concentration of uric acid reaches to a particular limit i.e. 11mg/dl, output of differential amplifier reaches 6.80V. At this voltage, output light switches from one port to the other. Thus, the output light intensity is being controlled by the voltage available at the output of differential amplifier, which in turn is calibrated with the concentration of uric acid through wheat stone bridge and a differential amplifier. So, with the help of proposed device, concentration of uric acid in serum can be calculated without need of any other device or measuring equipment.

Table 1: Variation of different parameters of uric acid concentration sensor

S. No.	Uric acid Conc. (mg/dl)	Non-linear refractive index $n \times 10^8 cm^2/W$	Electric field at output of PCF (V/m)	Power at output of PCF (mW)	Resistance (Ω)	Voltage at output of differential amplifier (V)	Electric field at first output of MZI
1	3	5.89	0.4472	0.49	75	0	0.04
2	5	8.84	0.4320	0.46	81	1.99	0.44
3	7	12.47	0.4195	0.44	88	3.98	0.78
4	9	14.65	0.4052	0.41	95	5.73	0.95
5	11	17.96	0.3950	0.39	102	6.80	0.99

Figure 5 shows the BPM simulation results for the proposed structure. From the results, it can be clearly seen that for 0 Volt applied to second electrode of MZI, light comes out of second output port of MZI. As the concentration of uric acid goes on increasing, light at second output port goes on decreasing and light at first output port goes on increasing simultaneously. As the concentration reaches its upper limit, all the light gets shifted to its first output port.

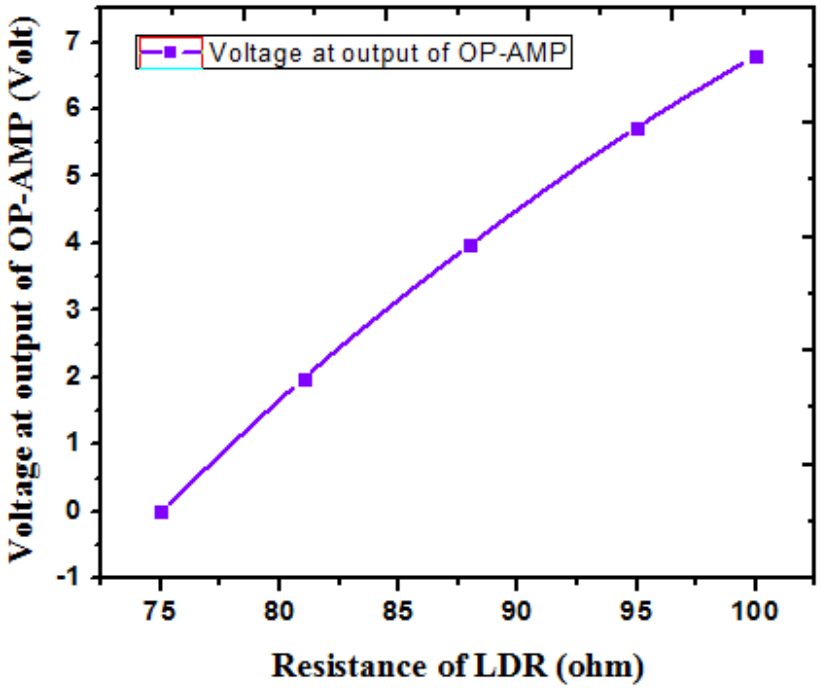

Fig. 4: Voltage at the output of differential amplifier with respect to resistance.

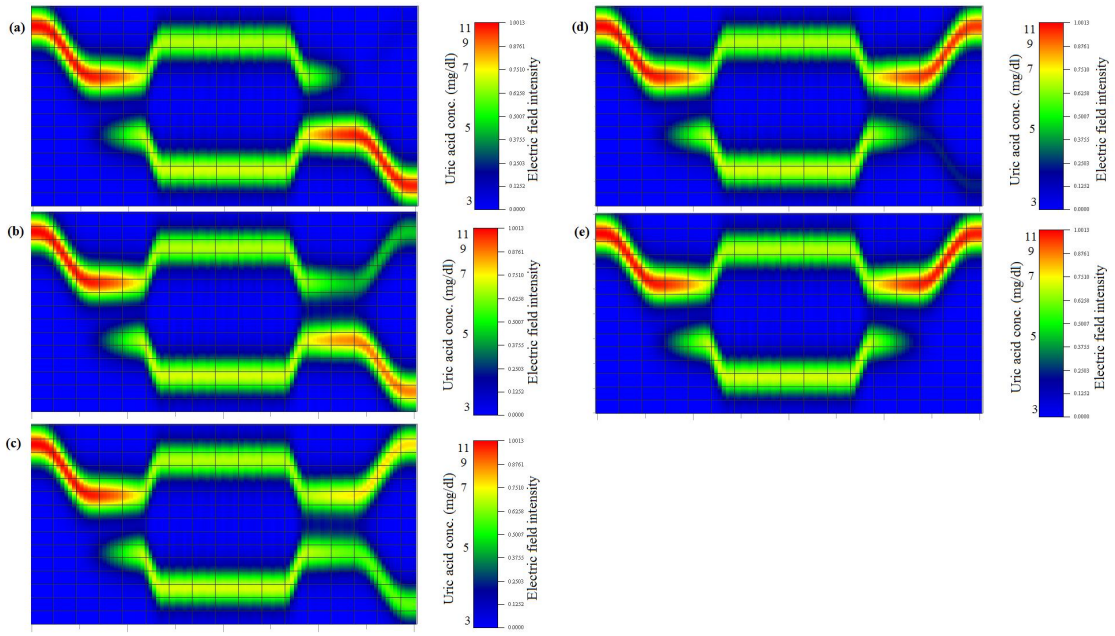

Fig. 5: OptiBPM simulation results for the uric acid concentration sensor.

3. CONCLUSION

In this work, a design of uric acid sensor is demonstrated using solid-core photonic bandgap fiber and electro-optic effect of Lithium Niobate ($LiNbO_3$) based MZI structure. The proposed design provides the direct value of the concentration of the uric acid in the blood; so, direct measurement of the uric acid concentration is possible at the output. The measurement is performed for a range of 8 mg/dl (from 3 mg/dl to 11 mg/dl). The sensitivity is at its best because of the novel applications of PCFs. By employing the differential amplifier appropriate voltage at the second electrode of the MZI can be provided precisely. The voltage at the second electrode of MZI, (and hence the output intensity of light at the first output port of MZI) is calibrated with the concentration of the uric acid to provide the direct output value. Hence the proposed device is very promising for biomedical sensing applications (uric acid in our case) using optical techniques.

Acknowledgement

This work is supported by the project entitled "Performance study of some WDM optical network components and design of optical switching devices" under the Faculty Research Scheme of DIT University (Ref. No.: DITU/R&D/2014/7/ECE) undertaken by Dr. Santosh Kumar. The authors would also like to thank Prof. K. K. Raina for encouragement and support during the present research work.

References:

[1] Dicaire, I., Rossi, A.D., Combrie, S. and Thevenaz, L., " Probing molecular absorption under slow-light propagation using a photonic crystal waveguide," Opt. Lett. 37, 4934-4936 (2012).

[2] Farrer, R.A., Previte, M.J.R., Olson, C.E., Peyser, L.A. and Fourkas, J.T., " Single-molecule detection with a two-photon fluorescence microscope with fast-scanning capabilities and polarization sensitivity," Opt. Lett. 24, 1832-1834 (1999).

[3] Jensen, J.B., Pedersen, L.H., Hoiby, P.E., Nielsen, L.B., Hansen, T.P., Folkenberg, J.R., Riishede, J., Noordegraaf, D., Nielsen, K., Carlsen, A. and Bjarklev, A., "Photonic crystal fiber based evanescent-wave sensor for detection of biomolecules in aqueous solutions," Opt. Lett. 29, 1974–1976 (2004).

[4] Jensen, J.B., Hoiby, P.E., Emiliyanov, G., Bang, O., Pedersen, L.H., and Bjarklev, A., "Selective detection of antibodies in microstructured polymer optical fibers," Opt. Express 13, 5883–5889 (2005).

[5] Ye, J.Y., Myaing, M.T., Thomas, T.P., Majoros, I., Koltyar, A., Baker, J.R., Wadsworth, W.J., Bouwmans, G., Knight, J.C., Russell, P.St.J. and Norris, T.B., "Development of a double-clad photonic crystal fiber based scanning microscope," Proc. SPIE 5700, 23-27 (2005).

[6] Xie, H., Pan, Y. and Fedder, G.K., "Endoscopic optical coherence tomographic imaging with a CMOSMEMS micromirror," Sens. Actuators 103, 237-241 (2003).

[7] Tran, P., Mukai, D., Brenner, M. and Chen, Z., "In vivo endoscopic optical coherence tomography by use of a rotational microelectromechanical system probe," Opt. Lett. 29, 1236-1238 (2004).

[8] Herz, P., Chen, Y., Aguirre, A., Schneider, K., Hsiung, P., Fujimoto, J., Madden, K., Schmitt, J., Goodnow, J. and Petersen, C., "Micromotor endoscope catheter for in vivo, ultrahigh-resolution optical coherence tomography," Opt. Lett. 29, 2261-2263 (2004).

[9] Liu, Y.,Liu, B., Feng, X.H., Zhang, W.G., Zhou, G., Yuan, S.Z., Kai, G.Y. and Dong, X.Y., "High-birefringence fiber loop mirrors and their applications as sensors," Appl. Opt. 44, 2382-2390 (2005).

[10] Kumar, S., Kumar, A., Raghuwanshi, S.K., "Implementation of an optical AND gate using Mach-Zehnder interferometers," Proc. SPIE 9131, Optical Modelling and Design III, SPIE Photonics Europe 2014, Brussels, Belgium, pp. 913120 (2014).

[11] Kumar, A., Kumar, S., Raghuwanshi, S.K., "Implementation of XOR/XNOR and AND Logic Gates using Mach-Zehnder interferometers," Optik 125, 5764-5767 (2014).

[12] Dimitriadou, E., Zoiros, K.E., "On the feasibility of ultrafast all-optical NAND gate using single quantum-dot semiconductor optical amplifier-based Mach-Zehnder interferometer," Opt. & Laser Technology 44, 1971-1981 (2012).

[13] Dimitriadou, E., Zoiros, K.E., "On the design of reconfigurable ultrafast all-optical NOR and NAND gates using a single quantum-dot semiconductor optical amplifier-based Mach–Zehnder interferometer," J. Opt. 14, 105401 (2012).

[14] Kumar, A., Kumar, S., Raghuwanshi, S.K., "Implementation of Full-adder and Full-subtractor based on Electro-optic Effect in Mach Zehnder interferometer," Optics Communication 324, 93-107 (2014).

[15] Kumar, S., Bisht, A., Singh, G., Choudhary, K., Sharma, D., "Implementation of Wavelength Selector based on Electro-optic Effect in Mach-Zehnder interferometers for High Speed Communications," Optics Communication, (2015) doi:10.1016/j.optcom.2015.03.069.